ELSEVIER

Chemical Engineering Journal 126 (2007) 79–85

Chemical Engineering Journal

www.elsevier.com/locate/cej

Steam activation of tyre pyrolytic carbon black: Kinetic study in a thermobalance

A. Aranda, R. Murillo, T. García, M.S. Callén, A.M. Mastral *

Instituto de Carboquímica, CSIC, M. Luesma Castan 4, 50018-Zaragoza, Spain

Received 11 July 2006; received in revised form 29 August 2006; accepted 30 August 2006

Abstract

Kinetic parameters for the steam activation of tyre pyrolytic carbon black have been determined by thermogravimetric analysis (TGA). Pyrolytic carbon black is a mainly macro and mesoporous material whose surface area can be improved via gasification to obtain microporous activated carbons. The pyrolytic carbon black sample was produced in an experimental-scale assembly where shredded tyre was pyrolysed under controlled conditions in a fixed bed reactor. Then, the activation of the resulting solid was studied by TGA using steam as activating agent. Kinetic regime was ensured fixing experimental conditions and therefore, avoiding internal and external mass transfer and heat transmission phenomena. Temperature (850–950 °C) and activating gas concentration (10–40 vol.%) were the influencing variables under study. This is the first time that the random pore model (RPM) has been used to fit experimental data of the activation of pyrolytic carbon black with steam. Excellent fittings have been obtained because of the special applicability of this model to predict the behaviour of solid–fluid reactive systems, in which the solid phase shows a porous structure. Reaction evolution has successfully been modelled, including the maximum reaction rate obtained in experimental results. Additionally, intrinsic kinetic parameters of the activation reaction–reaction order, activation energy and pre-exponential factor – were calculated.

Keywords: Tyre; Pyrolysis; Activated carbon; Random pore model; Kinetic modelling; Steam activation

1. Introduction

Nowadays, the disposal of waste materials supposes a worrying environmental problem as industrialised countries generate a large amount of residues. The trouble importance increases as most of those residues show high heterogeneity, which complicate their recycling in terms of environmental and economical feasibility. This is the case of waste tyres, which show even wider heterogeneity each day, as properties are improved by changing their formulation.

Tyres comprise more than 100 different substances. The main components are rubber (50 wt.%), fillers like carbon black or silica gel (25 wt.%), steel (10 wt.%), sulphur (1 wt.%), zinc oxide (1 wt.%) and many other additives like processing oil, plasticizers or vulcanisation accelerators [1]. It is estimated that 2.5 million tonnes per year are generated in the European Union, 2.5 million tonnes in North America and around 1 million tonnes in Japan [2]. The accumulation of tyre waste in open field results in an eyesore, potential health and environmental hazards – insect plagues, fires, etc. – large spaces occupied and a wastage of a valuable energy resource.

Several trials to reduce landfill disposal have been developed or are under study yet. Tyre recycling practices like retreading, grinding and using tyre as additive for sports tracks or roads asphalt have been performed. However, all of them have significant drawbacks or limitations [3]. Additionally, the heating value of tyres – around 28–37 MJ/kg [4] – is comparable to high rank coals, so thermal processes like combustion, pyrolysis and gasification have been considered to be attractive methods for recovering energy from scrap tyre.

Over the last years, tyre pyrolysis has received renewed attention because it could yield valuable products. Thus, the gas fraction could be used as fuel as it is mainly composed of CO, H_2 and light hydrocarbons [5]. On the other hand, the liquid product is a complex mixture of organic compounds of 5–20 carbon atoms with a very high proportion of aromatics [2]. After distillation, this liquid fraction could be used as heating oil or blended

Abbreviations: DR, Dubinin–Radushkevich equation; MVRM, modified volume reaction model; PSD, pore size distribution; RPM, random pore model; SCM, shrinking core model; TGA, thermogravimetric analysis; VRM, volume reaction model

* Corresponding author. Tel.: +34 976 733977; fax: +34 976 733318.
E-mail address: amastral@carbon.icb.csic.es (A.M. Mastral).

1385-8947/$ – see front matter © 2006 Elsevier B.V. All rights reserved.
doi:10.1016/j.cej.2006.08.031

Nomenclature

C	gasifying agent concentration (mol m^{-3})
E_a	activation energy (kJ mol^{-1})
k	intrinsic constant rate (m s^{-1})
k_0	pre-exponential factor in Ahrrenius equation ((mol/m^3)^n m s^{-1})
L_0	length of a system that is made by the random overlapping of cylindrical surfaces whose size distribution is $V_0(r)$ (m m^{-3})
n	reaction order
R	universal gas constant (8.314 J mol^{-1} K^{-1})
S_0	surface area of a system that is made by the random overlapping of cylindrical surfaces whose size distribution is $V_0(r)$ (m^2 m^{-3})
S_{BET}	surface area obtained by applying the BET equation to the N_2 adsorption isotherm (m^2 g^{-1})
$V_0(r)$	pore volume distribution
w_{ash}	sample ash weight (mg)
w_i	sample weight at any time (mg)
w_0	sample initial weight (mg)
X	solid fractional conversion
X_{exp}	solid experimental conversion

Greek symbols

ε_0	total volume of a system that is made by the random overlapping of cylindrical surfaces whose size distribution is $V_0(r)$
ψ	Bathia and Perlmuter structural parameter

with petroleum refinery streams to obtain automotive fuels [6]. Finally, the solid fraction could be used as solid fuel or low-grade carbon black. However, it is a product with high carbon content that makes it a suitable material for active carbon production [5,7]. Nowadays, the economical viability of tyre upgrading by pyrolysis clearly depends on the improvement of these products final properties and their commercial outlet.

According to this interest, many attempts have been carried out to generate activated carbons from waste tyres [8–15]. As pyrolytic tyre carbonaceous residue does not present remarkable superficial properties – around 60–80 m^2/g of surface area [10,15] – physical and/or chemical activation is widely used to improve its textural properties. After different activation methods [12,14], reported surface areas vary from 272 to 1117 m^2/g depending on solid conversion degree, activating agent, demineralization process, etc. The most common activating agents for the physical activation of pyrolytic carbon black are steam and carbon dioxide and it is generally accepted that steam is a more reactive gasifying agent than CO_2 [16,17]. Differences in the final surface areas of the activated carbon for the same conversion degree have been reported [17], finding that steam activation is two or three times faster than CO_2 activation.

Even though activated carbons are of interest in a wide range of application areas [11,13,15], and pyrolytic tyre derived solid activation has been carried out by several authors, kinetic studies for pyrolytic carbon black gasification have not been developed in depth. However, different models proposed for coal chars have been found suitable in understanding the gas–solid reaction kinetics [18–20]. Char-coal gasification experimental results have been interpreted by using the shrinking-core model (SCR), volume reaction models, combined models, intrinsic reactivity models with chemical kinetics and models that consider pore development (random pore model).

Regarding to the gasification kinetics of pyrolytic carbon black, few studies are available and most of them are focused on CO_2 activation. Lee and Kim [21] used the shrinking core model (SCM), the volume reaction model (VRM) and the modified volume reaction model (MVRM) to predict CO_2 pyrolytic carbon black activation from thermobalance experiments. Mastral and co-workers [15] first used the random pore model (RPM) to accomplish the kinetic modelling of pyrolytic carbon black in CO_2 gasification, obtaining the reaction kinetic parameters by thermogravimetric analysis. Different models (VRM, MVRM, changing grain size model and the RPM) were compared for experimental data fitting and the structural properties based model (RPM) showed the highest accuracy [22].

On the other hand, pyrolytic carbon black gasification data with steam as activating agent are scarce in the literature. Different values of activation energy are currently available; Cunliffe and Williams [8] obtained a value of 201 kJ/mol and, Merchant and Petrich [9] reported values ranging from 226 kJ/mol (low conversion data) to 153 kJ/mol (high conversion data). However, structural parameters influence and pore structure evolution remain unclear [17] and any scaling-up process design to obtain activated carbons must unavoidable be based on a deep kinetic knowledge. Thus, in this work, kinetic modelling of pyrolytic carbon black steam gasification has been developed. To the best of our knowledge this is the first time that the random pore model has been applied to obtain kinetic parameters from thermobalance experiments of pyrolytic carbon black steam gasification. In this model, structural parameters are considered and reaction rate and solid properties evolution are well described as theoretical and experimental data agreement evidenced.

1.1. Theory

It is well known that fluid–solid reactions are strongly influenced by solid structural properties, especially when the solid phase is a porous material. Therefore, a model developed in terms of pore size distribution (PSD) – unlike nonporous particle models – results suitable for char activation reaction modelling [15].

The random pore model (RPM) [23], takes into account the solid porosity including structural parameters calculated from the PSD. This model is able to predict a maximum in reaction rate when the structural evolution of the solid reaches certain values of the system parameters. Conversely, the SCM [24] and the VRM [25] cannot describe a maximum in reaction rate but predict a constant decrease of reaction rate. The main difference between the RPM and models that predict monotonically decreasing reaction rate is that, in the RPM, pore overlapping is considered. Pore shape is assumed cylindrical and supposed

to grow radially while reaction proceeds, instead of keeping initial volume. Initially, the cylinders growth causes an increase in total reaction surface, which means higher reaction rate. Finally, reaction progress brings about a neighbouring pore intersection. Due to pore overlapping, the reaction surface area is lower and, consequently, the reaction rate decreases.

The main RPM equations are as follows:

$$\frac{dX}{dt} = \frac{kC^n S_0}{(1-\varepsilon_0)}(1-X)\sqrt{1-\psi\ln(1-X)} \quad (1)$$

where X is the solid fractional conversion, k the intrinsic constant rate and C the gasifying agent concentration, n the reaction order. S_0, ε_0 and Ψ are structural parameters and they are calculated according to Eqs. (3)–(5):

$$S_0 = 2\int_0^\infty \frac{V_0(r)}{r}dr \quad (2)$$

$$\varepsilon_0 = \int_0^\infty V_0(r)dr \quad (3)$$

$$\psi = \frac{4\pi L_0(1-\varepsilon_0)}{S_0^2} \quad (4)$$

where $V_0(r)$ is the initial pore size distribution and L_0 is the porous system length at $t=0$:

$$L_0 = \frac{1}{\pi}\int_0^\infty \frac{V_0(r)}{r^2}dr \quad (5)$$

S_0, L_0 and ε_0 account for the surface area, length and total volume of a system that is made by the random overlapping of cylindrical surfaces whose pore size distribution is $V_0(r)$.

2. Experimental

Shredded tyre was supplied by Prosum Plus SL, a Spanish waste tyre recycling company. This tyre was pyrolysed in an experimental assembly specially designed to produce tyre char under controlled conditions. Once pyrolytic carbon black was obtained, thermobalance operational conditions were optimised to ensure kinetic regime in thermogravimetric experiments. Thus, this preliminary study included carrier gas flow, particle diameter, maximum temperature and sample weight. Finally, thermogravimetric analyses were carried out to obtain the kinetic parameters for the steam activation of pyrolytic carbon black.

2.1. Pyrolytic carbon black production and characterisation

Pyrolytic carbon black was produced in an experimental assembly which included a preheater for the carrier gas, a 2.4 cm internal diameter stainless steel fixed bed reactor followed by a condenser, a filter and, finally, a burner were pyrolysis gas products were burned. Additionally, flow and temperature controllers allowed the control of the system variables. Thus, 60 g of waste tyre, with a particle diameter <1 mm, were introduced in the reactor. Preheated nitrogen flows downwards at atmospheric pressure while the reactor reached 650 °C with a heating rate of 50 °C/min. Isothermality was kept for 60 additional minutes to achieve complete tyre conversion.

Char textural characterisation was accomplished by N_2 adsorption at 77 K, by using an ASAP 2000 (Micromeritics) apparatus. The sample surface area was calculated by applying the BET equation to the N_2 adsorption data and the total micropore volume was obtained by applying the Dubinin–Radushkevich equation (DR) to the nitrogen adsorption isotherm. The total pore volume was considered to be the volume of adsorpted N_2 at a relative pressure of 0.95. Analyses of mercury porosimetry were carried out in a Quantachrome POREMASTER GT (33/60). In this way, it was possible to calculate the pore size distribution for meso- and macropores.

2.2. Steam activation of pyrolytic carbon black

TGA experiments were performed in a Setaram TGC-85 thermobalance, prepared to use steam as activating agent. The inert gas–nitrogen – can enter the thermobalance straightforward or after having passed through a stainless steel water bubbler with a temperature controlled heater. Once the sample and the bubbler have reached the aimed temperature, reaction gas was passed through the thermobalance. The steam partial pressure was controlled by means of the bubbler temperature. Before starting steam activation, the sample temperature was risen to 900 °C and held for an hour under nitrogen atmosphere.

From preliminary experiments, optimum values of gas flow, average particle size, sample weight and maximum temperature were determined to avoid external and internal mass transfer phenomena and heat transfer control. Kinetic regime in thermobalance experiments was ensured with the following variable ranges: flow rates ranging from 2 to 3 m/s of N_2; temperature lower than 950 °C; sample weight ranging from 5 to 20 mg; and average particle size lower than 0.250 mm. Once operational conditions were fixed, temperature (850–950 °C) and steam percentage (10–40 vol.%) were varied to calculate intrinsic kinetic parameters.

All over this paper, experimental conversion (X_{exp}) has been calculated according to Eq. (6) where w_0 is the initial sample weight, w_i is the sample weight at any time and w_{ash} is the ash weight (the invariable weight after reaction):

$$X_{exp} = \frac{w_0 - w_i}{w_0 - w_{ash}} \quad (6)$$

3. Results and discussion

3.1. Tyre devolatilisation results

Reported results show that tyre rubber starts to decompose at 450 °C and this process is essentially completed at 500–600 °C [8]. In this work, tyre pyrolysis experiments were carried out at 650 °C with a heating rate of 50 °C/min. Even though heating rate affects to liquid–gas yields [8,26], no influence on solid yield has previously been reported. Total rubber degradation can be easily achieved and the final pyrolysis residue is mainly

Table 1
Proximate and ultimate analyses (as received basis) of tyre and tyre pyrolytic carbon black

Sample (wt.%)	Tyre	Pyrolytic carbon black
Moisture	0.64	0.22
Ash	4.88	9.51
Volatile matter	64.46	2.57
Fixed carbon	30.02	77.7
C	85.03	87.37
H	7.65	0.66
N	0.47	0.31
S	1.6	2.63

comprised of carbon black and mineral matter. In this research, once the final temperature was reached, isothermal conditions were kept for 60 additional minutes to ensure the complete volatile matter release in the sample. This fact was corroborated by proximate analysis, see Table 1. The pyrolysis resulting solid yield was 37 wt.%, which also agrees with several previous reported results [15,22,27]. Regarding to proximate analysis, the remarkable amount of ashes found in the char has also been observed in other studies, where ash percentage ranged from 10 to 15 wt.% [8,14]. These values were depending on the composition of the tyre feed, and specially, on the initial mineral matter of tyre (ZnO, SiO_2, etc.). Additionally, it can be observed that the char yield is slightly higher than the sum of fixed carbon and ash content of the original tyre. This issue is likely due to repolymerization reactions caused by pyrolytic charring of organic polymers [15].

Concerning to pyrolytic carbon black structure, it has been commented above that this material is mainly macroporous and mesoporous, with a very small contribution of microporosity to the total pore volume [15]. From mercury porosimetry (see Fig. 1), it was observed that the mean pore size distribution is centred in 50 nm, which agrees with Lin and Teng reported results [13].

The textural properties of pyrolytic carbon black are given in Table 2. It can be observed that the surface area calculated from the N_2 adsorption data by applying the BET equation [28] was 82 m^2/g, a typical value for chars prepared from waste tyre [15]. It is also reported in Table 2 that pyrolytic carbon black presents a negligible total microporosity. Therefore, it

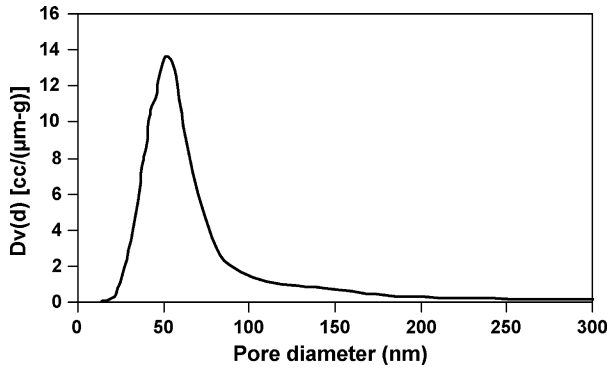

Fig. 1. Pyrolytic carbon black mercury porosimetry.

Table 2
Textural properties of tyre pyrolytic carbon black

S_{BET} (m^2/g)	82
Total pore volume (cm^3/g)	0.40
Total micropore volume (cm^3/g)	<0.01
Average pore size (nm)	50

Table 3
Random pore model structural parameters

Ψ	4.39
S_0 (m^2/m^3)	1.42×10^7
ε_0 (m^3/m^3)	0.243
L_0 (m/m^3)	9.34×10^{13}

can be assumed that the pore size distribution obtained from mercury porosimetry is representative of the material porosity to calculate RPM parameters. Thus, this pore size distribution will be used to calculate the RPM structural parameters (see Table 3).

3.2. Pyrolytic carbon black activation: flow rate influence

In all thermobalance experiments, a previous sample conditioning step was carried out at 900 °C for an hour under nitrogen atmosphere. During this step, an initial weight loss about 2 wt.% was observed. This fact was attributed to the elimination of the remaining high-molecular-weight volatile compounds from the char.

First, flow rate influence was studied in order to avoid external mass transfer and elutriation phenomena. Thus, flow rate was varied from 2 to 3 m/s whilst the rest of the variables were fixed (10 vol.% steam, 0.150 mm < particle diameter < 0.250 mm, 900 °C, 10 mg sample weight). It is observed in Fig. 2 that the reaction was not controlled by external diffusion whilst flow rate was between 2 and 3 m/s, as similar conversions were obtained. In the case of higher flow rates, elutriation phenomenon was observed (these results are not shown in Fig. 2), i.e. final weight data were much lower than the expected values according to proximate analysis.

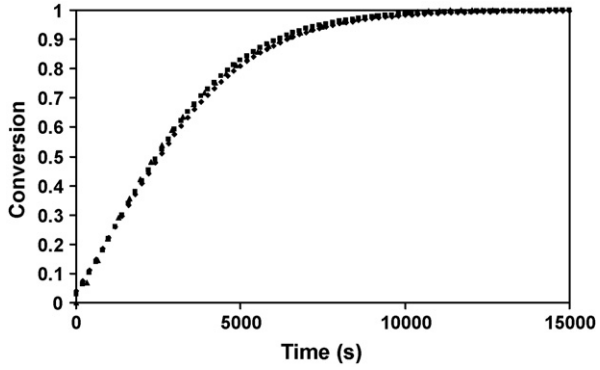

Fig. 2. Conversion vs. time for pyrolytic carbon black steam activation for different nitrogen flow. (■) 2 m/s; (▲) 2.5 m/s; (♦) 3 m/s.

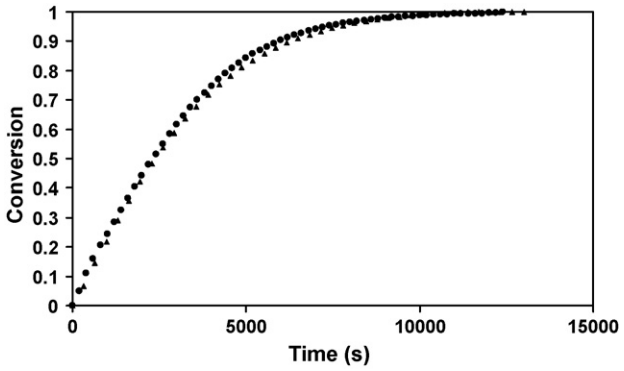

Fig. 3. Conversion vs. time for pyrolytic carbon black steam activation for different sample particle diameter. (●) $dp < 0.150$ mm; (▲) 0.150 mm $< dp < 0.250$ mm.

3.3. Pyrolytic carbon black activation: average particle size influence

Average particle size influence was also studied and experimental results are reported in Fig. 3. This Fig. 3 shows that average particle sizes lower than 0.250 mm avoided internal mass transfer restrictions. Thus, the remaining experiments were carried out with 0.150–0.250 mm particle diameter samples.

3.4. Pyrolytic carbon black: initial sample weight influence

Sample weight was fixed from the experimental results plotted in Fig. 4. When kinetic studies are performed, it is important to avoid mass transfer phenomena not only in the individual particles, but also in the sample bed because lower reaction rates would be measured and the kinetic parameters would be apparent. It can be observed that experimental data for sample weights of 5–20 mg did not show any remarkable influence. Experiments were carried out with 10–15 mg of initial sample weight because higher weight values were not allowed due to the thermobalance basket size.

3.5. Kinetic parameters

Once optimum conditions were determined, two experimental series varying steam concentration and process temperature were performed to obtain intrinsic kinetic parameters. In all experiments, heating rate value was fixed to 20 °C/min. It is worth to point out that it can be ruled out any influence of the heating rate during the conditioning step, as it has previously been reported [14].

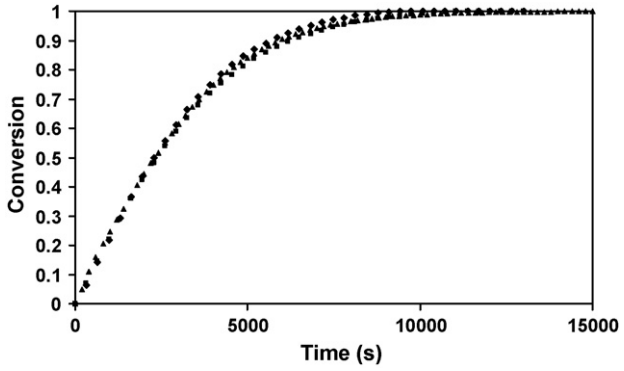

Fig. 4. Conversion vs. time for pyrolytic carbon black steam activation with different initial sample weight. (♦) 7 mg; (■) 10 mg; (▲) 20 mg.

Table 4
Conditions and fitted kC^n values for the experimental series carried out to obtain reaction order

T (°C)	H_2O (vol.%)	kC^n
900	13	7.4E−12
900	16	8.9E−12
900	26	1.043E−11
900	32	1.28E−11
900	39	1.45E−11
900	48	1.72E−11

According to Eq. (1), the reaction order can be obtained varying steam concentration whilst the rest of the parameters remain constant. Thus, (kC^n) values were obtained for different steam concentrations (see Table 4). Finally, the reaction order is obtained by plotting these parameters versus steam concentration, according to Eq. (7). Correlation coefficients higher than 0.98 were found with a reaction order of 0.6:

$$\mathrm{Ln}(kC^n) = \mathrm{Ln}(k) + n\,\mathrm{Ln}(C) \quad (7)$$

The activation energy (E_a) and the pre-exponential factor (k_0) were determined by performing experiments at five different temperatures (850, 875, 900, 925 and 950 °C) with a fixed steam concentration (26 vol.%) and the corresponding kC^n values were obtained (Table 5).

The pyrolytic carbon black has proven to be a very inert material under gasification conditions. Although steam gasification is a faster reaction than CO_2 gasification [15], high temperatures were also needed to achieve elevated kinetic constants. The activation energy and pre-exponential factor were calculated by the common Arrhenius representation (Eq. (8)) with excellent correlation coefficients between experimental and calculated data

Table 5
Conditions and fitted kC^n values for the experimental series carried out to obtain activation energy and pre-exponential factor

T (°C)	H_2O (vol.%)	kC^n
850	26	4.7E−12
875	26	6.15E−12
900	26	1.04E−11
925	26	1.42E−11
950	26	1.99E−11

Table 6
Kinetic parameters for steam pyrolytic carbon black activation

E_a (kJ/mol)	175.9
k_0 ((mol/m^3)^n m s^{-1})	3.7×10^{-4}
n	0.6

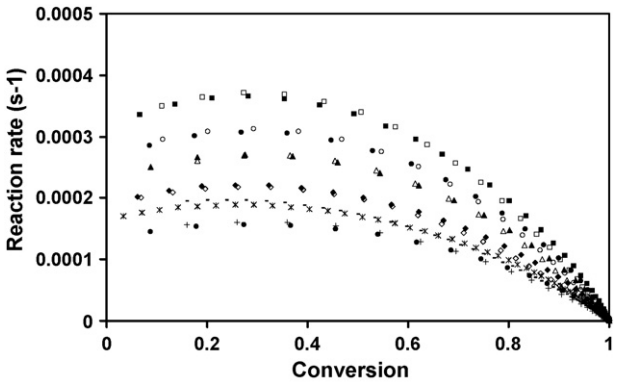

Fig. 5. Conversion vs. reaction rate for pyrolytic carbon black steam activation at different steam concentrations: (+) experimental 12 vol.%; (●) theoretical 12 vol.%; (−) experimental 14 vol.%; (*) theoretical 14 vol.%; (◊) experimental 18 vol.%; (♦) theoretical 18 vol.%; (△) experimental 27 vol.%; (▲) theoretical 27 vol.%; (◯) experimental 32 vol.%; (●) theoretical 32 vol.%; (□) experimental 40 vol.%; (■) theoretical 40 vol.%.

(higher than 0.99). Summarized results are shown in Table 6:

$$\mathrm{Ln}(K) = \mathrm{Ln}(k_0) + \left(\frac{-E_a}{R}\right)^* \left(\frac{1}{T}\right) \quad (8)$$

Finally, the gasification reaction rate of pyrolytic carbon black/steam may be deduced and used to calculate the theoretical one. The reaction rate is expressed according to Eq. (9):

$$\frac{dX}{dt} = 6.941 \times 10^3 \, e^{-21169/T} C^{0.6} (1 - X)\sqrt{1 - 4.39 \ln(1 - X)} \quad (9)$$

Figs. 5 and 6 compare the experimental and calculated reaction rates from RPM model for different steam concentrations and temperatures, respectively. It can be observed that RPM fits the experimental data accurately. It is worth to point out that the RPM was not only able to fit the conversion results but it was also able to predict the observed reaction rate maximum at conversion around 0.4 during the reaction. These maximum values agree with Bahtia and Perlmutter [23] and Lin and Teng [13] results. The maximum in reaction rate arises from two opposing effects. First, an initial pore growth occurs due to the gasification reaction. Second, the pore overlapping and coalescence takes place and large micropores are transformed into mesopores, decreasing the total reaction surface area [23]. Therefore, char gasification process must be controlled accurately when activated carbon with specific surface area is to be obtained.

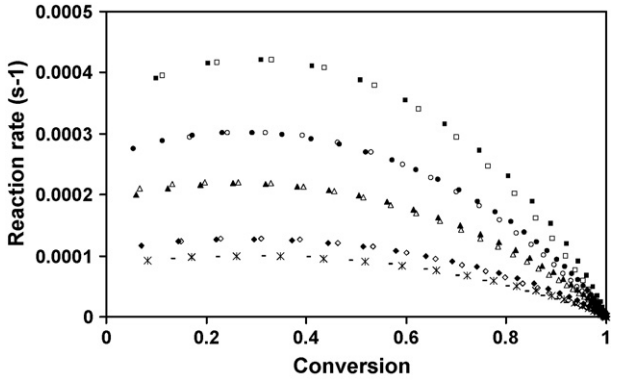

Fig. 6. Conversion vs. reaction rate for pyrolytic carbon black steam activation at different temperatures: (−) experimental 850 °C; (*) theoretical 850 °C; (◊) experimental 875 °C; (♦) theoretical 875 °C; (△) experimental 900 °C; (▲) theoretical 900 °C; (◯) experimental 925 °C; (●) theoretical 925 °C; (□) experimental 950 °C; (■) theoretical 950 °C.

Finally, only scattered data of activation energy for pyrolytic carbon black have been published. Cunliffe and Williams [8] reported 201 kJ/mol. Merchant and Petrich [9] obtained values ranging from 226 kJ/mol for low conversion to 153 kJ/mol for high conversion data. These values obtained in fixed bed reactor are similar to those obtained in this work where especial care has been taken in order to have kinetic control conditions. Therefore, in this study not only the kinetic control reaction regime assumed in Refs. [8,9] has been corroborated but also, previous models have been improved by incorporating morphological information for the calculation of kinetic parameters.

4. Conclusions

To the best of our knowledge, this is the first time that a pore size distribution based model has successfully been applied to obtain conclusive kinetic parameters for the steam gasification of pyrolytic carbon black. Kinetic regime has been ensured and the random pore model has fitted thermogravimetric results accurately. The deduced model not only was able to fit the pyrolytic carbon black conversion results, but also it is able to predict the maximum in reaction rate observed experimentally.

Acknowledgements

Authors would like to thank European Commission Contract RFC-CR-04006 for their partial financial support, the Spanish MEC, Juan de la Cierva Program, for Dr. T. García contract and to Drs. de Diego and Adánez the thermobalance use.

References

[1] S. Seidelt, M. Müller-Hagedorn, H. Bockhorn, J. Anal. Appl. Pyrolysis 75 (2006) 11–18.
[2] I. de Marco, M.F. Laresgoiti, M.A. Cabrero, A. Torres, M.J. Chomon, B. Caballero, Fuel Process. Technol. 72 (2001) 9–22.
[3] J.W. Jang, T.S. Yoo, J.H. Oh, I. Iwasaki, Conserv. Recycl. 22 (1998) 1–14.
[4] J.M. Ekmann, S.M. Smouse, J.C. Winslow, M. Ramezan, N.S. Harding, IEACR 90, 1996, 68 pp.
[5] A.M. Cunliffe, P.T. Williams, J. Anal. Appl. Pyrolysis 44 (2) (1998) 131–152.
[6] R. Murillo, A. Aranda, E. Aylón, M.S. Callén, A.M. Mastral, Ind. Eng. Chem. Res. 45 (2006) 1734–1738.
[7] M.F. Laresgoiti, I. De Marco, A. Torres, B. Caballero, M.A. Cabrero, M.J. Chomón, J. Anal. Appl. Pyrolysis 55 (1) (2000) 43–54.
[8] A.M. Cunliffe, P.T. Williams, Energy Fuels 13 (1) (1999) 166–175.
[9] A.A. Merchant, M.A. Petrich, AIChE J. 39 (8) (1993) 1370–1376.
[10] H. Teng, M.A. Serio, M.A. Wojtowicz, R. Bassilakis, P.R. Solomon, Ind. Eng. Chem. Res. 34 (1995) 3102–3111.
[11] C.M.B. Lehmann, M. Rostam-Abadi, M.J. Rood, J. Sun, Energy Fuels 12 (6) (1998) 1095–1099.
[12] R. Helleur, N. Popovic, M. Ikura, M. Stanciulescu, D. Liu, J. Anal. Appl. Pyrolysis 58–59 (2001) 813–824.
[13] Y.-R. Lin, H. Teng, Micropor. Mesopor. Mater. 54 (2002) 167–174.

[14] P. Ariyadejwanicha, W. Tanthapanichakoona, K. Nakagawab, S.R. Mukaib, H. Tamon, Carbon 41 (2003) 157–164.
[15] R. Murillo, M.V. Navarro, J.M. López, T. García, M.S. Callén, E. Aylón, A.M. Mastral, J. Anal. Appl. Pyrolysis 71 (2) (2004) 945–957.
[16] G.S. Miguel, G.D. Fowler, C.J. Sollars, Carbon 41 (2003) 1009–1016.
[17] E.L.K. Mui, D.C.K. Ko, G. McKay, Carbon 42 (2004) 2789–2805.
[18] R.C. Everson, H.W.J.P. Neomagus, H. Kasaini, D. Njapha, Fuel 85 (2006) 1067–1075.
[19] S. Kajitani, N. Suzuki, M. Ashizawa, H. Saburo, Fuel 85 (2006) 163–169.
[20] T. Morimoto, T. Ochiai, S. Wasaka, H. Oda, Energy Fuels 20 (2006) 353–358.
[21] J.S. Lee, S.D. Kim, Energy 21 (5) (1996) 343–352.
[22] R. Murillo, M.V. Navarro, J.M. Lopez, E. Aylon, M.S. Callen, T. Garcia, A.M. Mastral, Ind. Eng. Chem. Res. 43 (24) (2004) 7768–7773.
[23] S.K. Bhatia, D.D. Perlmutter, AIChE J. 26 (3) (1980) 379–386.
[24] O. Levenspiel, Chemical Reaction Engineering, 2nd ed., Wiley, 1975.
[25] S. Dutta, C.Y. Wen, Ind. Eng. Chem. Process. Des. Dev. 16 (1) (1977) 20–30.
[26] A.A. Merchant, M.A. Petrich, Chem. Eng. Commun. 63 (1992) 118–251.
[27] A.M. Mastral, R. Murillo, M.S. Callen, T. Garcia, C.E. Snape, Energy Fuels 14 (4) (2000) 739–744.
[28] S. Brunauer, P.H. Emmett, E.J. Teller, J. Am. Chem. Soc. 60 (1938) 309–319.